

## Stable phases of iron at terapascal pressures

This article has been downloaded from IOPscience. Please scroll down to see the full text article.

2009 J. Phys.: Condens. Matter 21 452205

(<http://iopscience.iop.org/0953-8984/21/45/452205>)

View [the table of contents for this issue](#), or go to the [journal homepage](#) for more

Download details:

IP Address: 38.107.179.212

The article was downloaded on 22/02/2012 at 13:33

Please note that [terms and conditions apply](#).

## FAST TRACK COMMUNICATION

# Stable phases of iron at terapascal pressures

Chris J Pickard<sup>1</sup> and R J Needs<sup>2</sup><sup>1</sup> Department of Physics and Astronomy, University College London, Gower Street, London WC1E 6BT, UK<sup>2</sup> Theory of Condensed Matter Group, Cavendish Laboratory, J J Thomson Avenue, Cambridge CB3 0HE, UK

Received 6 August 2009, in final form 5 October 2009

Published 21 October 2009

Online at [stacks.iop.org/JPhysCM/21/452205](http://stacks.iop.org/JPhysCM/21/452205)**Abstract**

We have used density-functional-theory methods to study phases of iron at terapascal (TPa) pressures. Hexagonal-close-packed (hcp) iron is stable from below 0.1 TPa to multi-TPa pressures, where we find a window of 7–21 TPa in which the face-centred-cubic (fcc) phase is slightly more stable. At 34 TPa we find a transition to a body-centred-tetragonal (bct) phase, which is a small distortion of the body-centred-cubic (bcc) structure. The bcc phase also becomes more stable than the hcp above 35 TPa. The bct and bcc phases become considerably more stable than hcp and fcc at even higher pressures, and we expect this result to hold at high temperatures.

(Some figures in this article are in colour only in the electronic version)

**1. Introduction**

Diamond-anvil-cell experiments [1] have achieved static compressions of up to about 350 GPa (=0.35 TPa), which is approximately the pressure at the centre of the Earth. Much higher pressures have been achieved in dynamical shock-wave experiments driven by conventional chemical explosives, gas guns, a Z-pinch, high-power lasers and underground nuclear explosions. Pressures of more than 10 TPa have been achieved in laser-driven shock-wave experiments and, with strong pre-compression of the samples and other advances, pressures up to 100 TPa might be achieved [2]. Similar pressures are expected to be achieved in laser-driven shock-wave experiments at the National Ignition Facility (NIF) [3].

The behaviour of materials under extreme conditions of pressure and temperature is of fundamental and technological interest. Iron is the most abundant element in the universe with an atomic number greater than 20 (in terms of either total mass or number of atoms). Iron is an important element in planetary science. The core of the Earth is largely composed of iron, with a liquid outer core and a solid inner core. There has been much interest in extrasolar planets (also known as exoplanets), several hundred of which have been discovered so far [4]. Exoplanets may be rather diverse in character, and their chemical compositions may vary widely. Reasonable

suppositions about the nature of an exoplanet may be made by combining the experimental observations of quantities such as mass and radius with a knowledge of the planets of the Solar System and the cosmic abundances of the elements. Jupiter is the most massive planet in the Solar System with a central pressure of roughly 7 TPa. Exoplanets of more than ten times the mass of Jupiter have been reported [4], and it is reasonable to suppose that some exoplanets may have iron-rich cores at pressures of tens of TPa or more. Understanding massive exoplanets will therefore require the study of materials at extremely high pressures and temperatures [2].

Fundamental thermodynamical properties of materials are described by the equation of state, which gives the equilibrium relationship between the pressure, volume and temperature. The equation of state of iron has been the subject of numerous experimental and theoretical investigations. Diamond-anvil-cell experiments have yielded a great deal of information about the equation of state of iron up to pressures of about 300 GPa [5, 6]. Under ambient conditions iron is ferromagnetic and adopts a body-centred-cubic (bcc) structure (the  $\alpha$  phase). Compression at ambient temperature induces a structural phase transition to a hexagonal-close-packed (hcp)  $\epsilon$  phase at 12–15 GPa, which is stable up to at least 300 GPa [5]. The structure of iron under the conditions within the Earth's solid inner core is highly controversial. First-principles or *ab initio*

density-functional-theory (DFT) calculations at core pressures and temperatures indicate that the hcp phase is a little more stable than bcc [7]. Other DFT calculations have suggested that face-centred-cubic (fcc) iron may be stable under inner core conditions [8]. As a further complication, the Earth's core contains a few per cent of atoms other than iron, which may be sufficient to stabilize the bcc structure [7].

Iron has been investigated at pressures much greater than those at the centre of the Earth using shock-wave techniques. Batani *et al* [9] reported laser-driven shock-wave data for the equation of state of iron at pressures up to 4.5 TPa. Trunin *et al* [10] reported shock-wave data for iron at pressures up to 10 TPa generated in an underground nuclear explosion, while a data point from a similar study at 19.1 TPa is reported in [11]. Experiments planned for the NIF aim to study iron at pressures beyond 100 TPa [3]. Investigations of iron at TPa pressures are expected to yield new information about the thermodynamics of iron and various other properties including its crystalline structures, which will be relevant to the study of exoplanets and to shock-wave studies.

## 2. *Ab initio* DFT calculations and stability of the phases

We have studied iron at very high pressures and temperatures using *ab initio* DFT methods. Our calculations were performed with the CASTEP plane-wave code [12], ultrasoft pseudopotentials [13] and the Perdew–Burke–Ernzerhof (PBE) generalized gradient approximation (GGA) density functional [14]. We have considered pressures up to 50 TPa, where the volume per iron atom is only about 1/8 of that at ambient conditions. Such an enormous compression provides a severe test of the accuracy of pseudopotential methods. We used pseudopotentials with the 3s, 3p, 4s and 3d orbitals treated explicitly. It is very important to include the 3s and 3p orbitals explicitly as their band dispersion is of a similar magnitude to that of the 3d orbitals at pressures of more than about 10 TPa. Ultrasoft pseudopotentials with core radii of 2 au are normally satisfactory for iron at low pressures, but much smaller core radii are required at multi-TPa pressures. We tested various pseudopotentials with core radii in the range 1.1–1.4 au, finding a pseudopotential core radius of 1.2 au to be sufficient to converge the calculations so that the resulting numerical errors in the enthalpy differences plotted in figure 1 are small on the scale of the figure. This core radius is sufficiently small to ensure that the pseudopotential cores on different atoms barely overlap even at 50 TPa, and we used this pseudopotential to obtain all of the results reported here. We also tested the effects of including the 2s and 2p orbitals in the pseudopotential explicitly, but the results were almost unchanged. This is to be expected as the 2p orbitals lie some 600 eV below the 3s orbitals.

Searches for candidate high-pressure phases were performed by combining *ab initio* methods with ‘random structure searching’ in the ‘AIRSS’ approach, which has proved very successful [15–18]. A set of randomly generated structures are relaxed to minimize their enthalpies at a chosen pressure. We performed searches with 4, 6, 8 or 10 atoms per unit cell

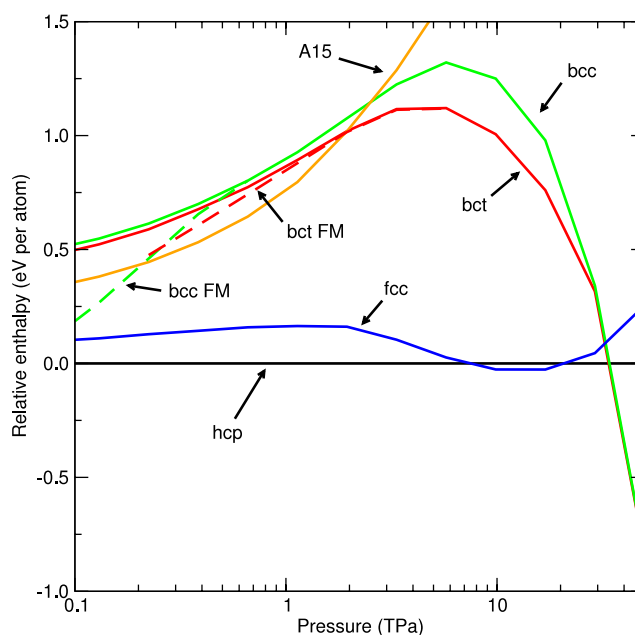


**Figure 1.** Pressure dependence of the enthalpies of various phases of iron with respect to the hcp phase. The dashed lines denote ferromagnetic (FM) phases and the solid lines denote non-magnetic phases.

at 30 TPa, and we also performed a number of searches at 10 TPa. For the searches we used a plane-wave basis set cutoff of 700 eV and the Brillouin zone integrals were evaluated using a  $k$ -point grid of spacing  $2\pi \times 0.07 \text{ \AA}^{-1}$ . The structures of interest were further relaxed at a higher level of accuracy consisting of a basis set cutoff of 1000 eV and a  $k$ -point grid spacing of  $2\pi \times 0.03 \text{ \AA}^{-1}$ . For the bcc structure, which has one atom per cell, this corresponds to about 6000  $k$ -points at 0.1 TPa and 30 000  $k$ -points at 50 TPa. The various searches produced the standard close-packed structures, such as fcc, hcp, a close-packed body-centred-tetragonal (bct) structure and the A15 structure, but we found no other energetically competitive phases. These searches did, however, generate the important negative result that, over the pressure range 0–50 TPa, only the standard high-symmetry structures need be considered. This result may not appear surprising, but it should be remembered that there are by now numerous examples of elements which adopt close-packed structures at low pressures but transform into more open structures (with shorter bond lengths) at higher pressures [19]. At zero temperature the most stable phase at each pressure is the one with the lowest enthalpy, so that the predicted phase transitions can be read off from figure 1. A number of DFT studies of iron have been performed up to pressures of a few hundred gigapascals and our results agree with the consensus that has arisen from previous work [20–27]. At low pressures a ferromagnetic bcc phase is the most stable, in agreement with experiment. As the pressure is increased a transformation to hcp is predicted, in agreement with experiment, although the calculations indicate antiferromagnetic spin ordering, which has not been observed experimentally. Magnetic spin ordering is not predicted to be energetically favourable at very high pressures. The A15 phase is lower in enthalpy than bcc over quite a wide range of

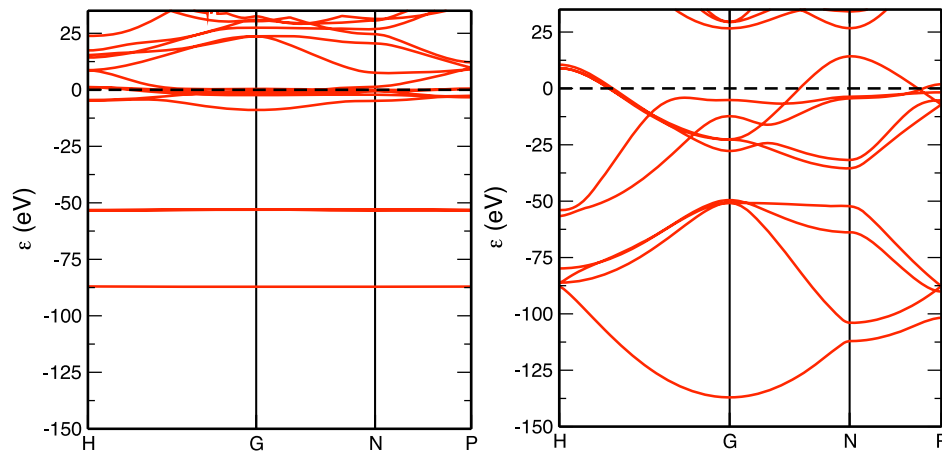


**Figure 2.** Band structures of (non-magnetic) bcc iron at zero pressure (left) and 30 TPa (right). The Fermi energies are at zero energy.

pressures, although it is not as well packed as the other phases and it becomes unfavourable at pressures above a few TPa. We predict a window of stability for the fcc phase in the pressure range 7–21 TPa, although the enthalpies of fcc and hcp are very close in this region. At around 10 TPa the enthalpies of the bcc and bct phases drop rapidly with respect to fcc and hcp, with a transition to bct occurring at 34 TPa. At 34 TPa the  $c/a$  ratio of the bct phase of 0.95 indicates only a small distortion from the bcc structure which corresponds to  $c/a = 1$ , and the distortion decreases with further compression. The bcc phase becomes more stable than hcp above 35 TPa. The downwards slopes of the bct/bcc curves in figure 1 above  $\sim 20$  TPa indicates that the bct and bcc phases are denser than hcp and fcc. At the phase transition at 34 TPa, the density of bct/bcc is about 0.6% larger than that of hcp.

### 3. Electronic structures of the phases at TPa pressures

The calculated band structures of non-magnetic bcc iron at 0 and 30 TPa are shown in figure 2. At low pressures the electronic configuration of the iron atoms can be described as  $3d^64s^2$ , and the 3s and 3p bands which lie at about  $-87$  eV and  $-53$  eV, respectively, are very narrow and do not play a significant role in the bonding. The 3s and 3p bands widen under pressure, and begin to overlap with each other at about 16 TPa, while the 3p and 3d bands begin to overlap at about 23 TPa. The 4s orbitals are much larger than the 3d orbitals, so that under compression they move to higher energies compared with the 3d bands. Charge consequently drains from the 4s bands into the 3d bands, a process which is completed at around 17 TPa, and the electronic configuration becomes  $3d^84s^0$ . A similar phenomenon has been described in Ni, where insulating behaviour is predicted at about 34 TPa because the transfer of the 4s electrons into the 3d bands leads to a full 3d shell [28].

Similar changes in the band structures occur in the other close-packed structures. The band structure of the bct phase is very similar to that of bcc, but the changes in the band structures described in the previous paragraph occur

at somewhat higher pressures in the fcc and hcp phases, presumably because the nearest-neighbour distance is larger. The electronic density of states (e-DoS) of bct is similar to that of bcc and the e-DoS of fcc is similar to that of hcp. The e-DoS of bcc at 30 TPa shows considerably more structure than those of hcp and fcc, as they do at zero pressure, although the changes from the zero-pressure e-DoS are substantial. Deegan [29] and Pettifor [30] showed that the electronic band structure energy determines, to a good approximation, the energy difference between close-packed structures at low pressures. This result also holds at TPa pressures. The band structure energies of the fcc and hcp phases are lower than those of bcc for volumes larger than about  $3.75 \text{ \AA}^3/\text{atom}$ , but at smaller volumes the band structure energy of bcc is lower. A volume of  $3.75 \text{ \AA}^3/\text{atom}$  corresponds to a pressure of about half the full *ab initio* transition pressure of 34 TPa.

A more detailed appreciation of the electronic structures of the phases can be obtained by studying the components of the total enthalpies. The total enthalpy  $H$  can be written as

$$H = T + E_H + E_{XC} + E_{Ps} + E_{Ew} + pV, \quad (1)$$

where  $T$  is the kinetic energy,  $E_H$  is the Hartree energy,  $E_{XC}$  is the exchange–correlation energy,  $E_{Ps}$  is the pseudopotential energy,  $E_{Ew}$  is the ion–ion electrostatic Ewald energy and  $pV$  is the pressure multiplied by the volume. The enthalpies of bcc and fcc phases with respect to those of hcp, and their components, are given in table 1 in the region of the transition to bct. Constraining the volumes of the bcc and fcc phases to equal that of hcp changes the individual components substantially, but the total enthalpies are not much affected. We make our comparisons at constant volume to eliminate the contribution to the enthalpy differences from the  $pV$  term. The enthalpy components of the bct phase are not shown in table 1, but they are very similar to those for bcc. The enthalpy components of the hcp and fcc phases are similar, while those of bcc are rather different, as expected because the local structures of the 12-fold-coordinated hcp and fcc phases are similar although they differ from that of the 8-fold-coordinated bcc phase. The main difference between the enthalpy components of the bcc/bct phases and the hcp/fcc

**Table 1.** Components of the enthalpy (in eV/atom) of phases of iron with respect to those of the hcp phase ( $X - X_{\text{hcp}}$ ). The entries labelled hcp, fcc and bcc are for a pressure of 29.1 TPa, where hcp is the most stable phase, and the entries fcc@hcp and bcc@hcp are results for fcc and bcc at the same volume as hcp.

Structure	$H$	$T$	$E_H$	$E_{XC}$	$E_{Ps}$	$E_{Ew}$	$pV$
hcp	0.00	0.00	0.00	0.00	0.00	0.00	0.00
fcc	0.05	0.00	0.93	-0.11	-2.05	1.06	0.22
bcc	0.34	-0.57	-2.85	-0.53	15.27	-9.36	-1.61
fcc@hcp	0.05	0.34	0.76	-0.18	-0.68	-0.19	0.00
bcc@hcp	0.35	-3.00	-1.60	-0.01	5.44	-0.48	0.00

phases is that the pseudopotential energy of bcc/bct is higher, while the kinetic and Hartree energies are lower. The iron pseudopotential is strongly attractive in all channels, and the larger pseudopotential energy of bcc/bct arises from a redistribution of charge away from the ionic cores. The resulting charge density is smoother and so the kinetic and Hartree energies are lower. This is consistent with the observation that the d-orbital charge density in the bcc structure has six lobes which point towards the centres of the faces of the cube and the second-nearest neighbours, while the d orbitals of the hcp and fcc structures do not fill space so well. The conclusions drawn from our analysis of the components of the electronic enthalpy are valid over a wide range of pressures from well below the transition to bct at 34 TPa to beyond 50 TPa.

We have calculated the harmonic vibrational modes of the bcc, hcp and fcc phases at several pressures. The largest vibrational frequencies of each structure increase with pressure, being about  $3000 \text{ cm}^{-1}$  ( $\equiv 4300 \text{ K}$ ) at 10 TPa, rising approximately linearly with pressure to about  $4300 \text{ cm}^{-1}$  ( $\equiv 6200 \text{ K}$ ) at 30 TPa. The conditions likely to exist in the deep interiors of massive planets of one or more Jupiter masses are, very roughly, temperatures of  $10^4$ – $10^5 \text{ K}$  with associated pressures of  $10^1$ – $10^3 \text{ TPa}$ . A classical description of the statistics of the vibrational modes of iron is justified in the cores of massive planets in the 10–30 TPa pressure range we have studied, and beyond. The harmonic vibrational free energies of the phases evaluated at finite temperatures actually favour the bcc phase over the hcp and fcc phases in the pressure range  $10^1$ – $10^3 \text{ TPa}$ , leading to a further stabilization of bcc at high pressures and temperatures. We have not, however, studied the anharmonic vibrational contributions which will be substantial. We have also investigated the effects of electronic excitations at finite temperatures. The changes in the free energies from thermal excitations are quite large at  $10^4$ – $10^5 \text{ K}$  temperatures and multi-TPa pressures, but the effects largely cancel between phases, and the overall effect on the relative stabilities of the phases is not large.

#### 4. Conclusion

In conclusion, we have used DFT methods to study phases of iron at TPa pressures. We performed computational searches which predict that only the standard high-symmetry phases need be considered, although we did find that the A15 phase, which has normally been neglected in studies of

iron, is competitive up to a few TPa. Our static-lattice zero-temperature DFT calculations showed a transition from hcp to fcc and back to hcp at TPa pressures, although the enthalpies of hcp and fcc are very similar in this pressure range, before an emphatic return to a bct phase at 34 TPa, which is a small distortion of bcc. The predicted stability of the bct/bcc phase at very high pressures is expected to be robust to the inclusion of finite-temperature effects.

#### Acknowledgment

The authors were supported by the Engineering and Physical Sciences Research Council (EPSRC) of the United Kingdom.

#### References

- [1] Jayaraman A 1983 *Rev. Mod. Phys.* **55** 65
- [2] Jeanloz R, Celliers P M, Collins G W, Eggert J H, Lee K K M, McWilliams R S, Brygoo S and Loubeyre P 2007 *Proc. Natl Acad. Sci.* **104** 9172
- [3] <https://lasers.llnl.gov/>
- [4] *The Extrasolar Planets Encyclopaedia* <http://exoplanet.eu/>
- [5] Mao H-K, Wu Y, Chen L C, Shu J F and Jephcoat A P 1990 *J. Geophys. Res.* **95** 21737
- [6] Dewaele A, Loubeyre P, Occelli F, Mezouar M, Dorogokupets P I and Torrent M 2006 *Phys. Rev. Lett.* **97** 215504
- [7] Vöcadlo L, Alfè D, Gillan M J, Wood I G, Brodholt J P and Price G D 2003 *Nature* **424** 536
- [8] Mikhaylushkin A S, Simak S I, Dubrovinsky L, Dubrovinskaja N, Johansson B and Abrikosov I A 2007 *Phys. Rev. Lett.* **99** 165505
- [9] Batani D, Morelli A, Tomasini M, Benuzzi-Mounaix A, Philippe F, Koenig M, Marchet B, Masclat I, Rabec M, Reverdin Ch, Cauble R, Celliers P, Collins G, Da Silva L, Hall T, Moret M, Sacchi B, Baclet P and Cathala B 2002 *Phys. Rev. Lett.* **88** 235502
- [10] Trunin R F, Podurets M A, Popov L V, Moiseev B N, Simakov G V and Sevastyanov A G 1993 *Sov. Phys.—JETP* **76** 1095
- [11] Trunin R F 1994 *Phys.—Usp.* **37** 1123
- [12] Clark S J, Segall M D, Pickard C J, Hasnip P J, Probert M I J, Refson K and Payne M C 2005 *Z. Kristallogr.* **220** 567
- [13] Vanderbilt D 1990 *Phys. Rev. B* **41** 7892
- [14] Perdew J P, Burke K and Ernzerhof M 1996 *Phys. Rev. Lett.* **77** 3865
- [15] Pickard C J and Needs R J 2006 *Phys. Rev. Lett.* **97** 045504
- [16] Pickard C J and Needs R J 2007 *Nat. Phys.* **3** 473
- [17] Pickard C J and Needs R J 2007 *Phys. Rev. B* **76** 144114
- [18] Pickard C J and Needs R J 2008 *Nat. Mater.* **10** 757
- [19] McMahon M I and Nelmes R J 2006 *Chem. Soc. Rev.* **35** 943
- [20] Steinle-Neumann G, Stixrude L, Cohen R E and Gülsersen O 2001 *Nature* **413** 57
- [21] Steinle-Neumann G, Stixrude L and Cohen R E 2004 *Proc. Natl Acad. Sci. USA* **101** 33
- [22] Steinle-Neumann G, Cohen R E and Stixrude L 2004 *J. Phys.: Condens. Matter* **16** 1109
- [23] Friák M and Šob M 2008 *Phys. Rev. B* **77** 174117
- [24] Belonoshko A B, Dorogokupets P I, Johansson B, Saxena S K and Koci L 2008 *Phys. Rev. B* **78** 104107
- [25] Vöcadlo L, Wood I G, Alfè D and Price G D 2008 *Earth Planet. Sci. Lett.* **268** 444
- [26] Qiu S L, Apostol F and Marcus P M 2008 *J. Phys.: Condens. Matter* **20** 345233
- [27] Sola E, Brodholt J P and Alfè D 2009 *Phys. Rev. B* **79** 024107
- [28] McMahan A K and Albers R C 1982 *Phys. Rev. Lett.* **49** 1198
- [29] Deegan R A 1968 *J. Phys. C: Solid State Phys.* **2** 763
- [30] Pettifor D G 1972 *Metallurgical Chemistry* ed O Kubaschewski (London: HMSO)